Investigating the Behaviour of a Home-Made Pendulum Based on the Damped Harmonic Oscillation Model

Sara Parvaresh Rizi | PHY180

INTRODUCTION

The pendulum is an excellent model for exploring principles of oscillatory motion, with its quality factor (Q factor or Q) and period being key parameters of interest. This report examines these parameters by testing a pendulum with a mass of 14.141 g and varying string lengths.

The Q factor, representing the frictional damping, can be attained by theoretical calculations of Q=$\pi * \frac{\tau}{T}$, where T is the period, and τ is attained by the damped harmonic motion model $\theta(t) = \theta_0 e^{-t/\tau} \cos\left(2\pi \frac{t}{T} + \emptyset_0\right)$, where t is time, T is period, and $\emptyset_0$ is the phase constant (Wilson, 2024a). By counting oscillations until the pendulum stopped, I experimentally obtained Q=163±1, while the theoretical damped harmonic motion model predicted Q=166±4, showing close agreement for a 0.4000 m string length. Due to this consistency, the counting method for Q factor was chosen to investigate the pendulum's relationship with length in the report.

A proposed model for the period of a pendulum is T=$T_0(1 + B\theta_0 + C\theta_0^2)$, where T is the period of the pendulum, T_0 is the initial period and $\theta_0$is the initial angle of release, and B and C are scalar coefficients (Wilson, 2024a). If B and C are experimentally 0, then there is no dependence between the period of the pendulum and its initial angle. However, as the initial angle of release increases, the approximation becomes less accurate, leading to deviations in the observed period. In this experiment, while B was -0.001±0.001, C was 0.061±0.003. This implied that though there is no asymmetry in the pendulum from B, there is some dependence for the period and the initial angle of release from C, where if the angle is less than -0.257 or greater than 0.257 radians, then there is a dependence. Consequently, small-angle experiments were conducted with angles inside this range to determine the relationship between Q factor and pendulum length.

Additionally, the period of a pendulum can also be described by the equation T=$2\sqrt{L}$, where T represents the period and L is the length of the pendulum (Wilson, 2024a). By plotting varying lengths of a pendulum against its period, I attained the equation T = (2.3±0.1)$L^{0.46\pm0.04}$, which is partly consistent with the model.

Lastly, it was found that the Q factor does depend on the length of the pendulum, and I propose that this relationship can be modelled using an exponential decay function, of Q = (127.21±0.01)$L^{-0.26\pm0.01}$.

METHODS

To build the pendulum, I took around 2m of thread, to ensure there was enough to later have an adjustable length. I chose a bouncy ball (14.141g) as my mass because it was dense and relatively small, which helped reduce air resistance and minimized frictional effects, making it ideal for this experiment *(see Figure 1a and Figure 1b).* To secure the ball, I wrapped it thoroughly with thread, so it remained attached during its motion, to reduce uncertainties due to detachment or slipping.

Figure 1a. A bouncy ball of mass 14.141 g hangs by a 0.4000 m string over a pencil that extends 3.00 cm off the edge of a table. A protractor is taped behind the pendulum to measure angular displacement.

Figure 1b. A bouncy ball of mass 14.141g wrapped with 2.000m of thread. The thread is wrapped around the tip of a pencil and around the bouncing ball so that it is 0.4000cm. A protractor is also visible.

After measuring the mass of the ball, including the wrapped string, I taped a pencil to the edge of a desk. This was to ensure that the surface of the desk would hold up the pendulum and that there was enough space under it for the pendulum's motion. As well, the tip of the pencil protruded a few centimetres away from the edge of the desk, so the pendulum had freedom of movement and did not hit the top of the surface. I wrapped the other end of the thread around the tip of the pencil and kept wrapping until the desired length for the pendulum. I tied a knot where the thread met the pencil so that when the ball hung down, the thread went directly down the centre of the rod *(see Appendix A image 2).* This controlled the pendulum's pivot point, minimized potential collisions, and reduced asymmetry in the design. More specifically, this design choice reduced uncertainty in measuring angles from the pivot point of the pendulum, because it ensured the pendulum reached the same height, without asymmetry, on both sides of motion.

I taped a protractor to the top of the desk so that 90º faced straight down, 0º was on the right of the pendulum (positive side) and 180º was on the left (negative side).

PROCEDURES

1. *Period vs. Angle Data*

To ensure an adequate range of data points and account for asymmetry, I selected 4-5 angles on both positive and negative sides of the pendulum that are between 0 and 90º, at 15° intervals (i.e., 15°, 30°, 45°, 60°). For each angle, I recorded four videos and counted for 5 oscillations, then divided the total time by five to calculate the period of a single oscillation. During data analysis, the angles were converted from degrees to radians for consistency in units.

2. *Amplitude vs. Time Data*

I chose an angle to release the pendulum at, that was sufficiently large to record its motion for a long time, and that is not 90º. Although my intended release angle was 60°, re-evaluation of the footage showed it to be approximately 60.70°. I recorded the motion of the pendulum at that release angle until it seemed to have reached a constant angle at which it oscillated. Using the Tracker app, I tracked the pendulum's angle (radians) against time (seconds), which I then fit to an exponential decay function (see *Equation 1, Appendix D*) to model the damped harmonic motion (Wilson, 2024a).

3. *Manual Q factor (counting method)*

I released the pendulum at the same angle 4 times on both the positive and negative sides. The Q was measured by counting the number of oscillations it took for the pendulum to reach an amplitude of around 46% ($e^{-\pi/4}$) of the initial angle and then multiplying that number by 4 (*see Table 1 in Appendix B*).

4. *Period vs. Pendulum length data*

Using a phone camera, I recorded the time it took for the pendulum to undergo 5 oscillations, then divided this time by 5 to get the time for one oscillation. To minimize uncertainties due to angle dependence, I consistently released the pendulum from an angle of 14.5°, which is small enough to assume a nearly constant period (*see Appendix E)*. I conducted five trials for each length, starting with an initial length of 0.4000 m and decreasing by 0.0500 m with each trial. Given that the pendulum was determined to be symmetric (*see Figure 2a*), trials were performed only on the positive side. This data was plotted on a log-log plot, and a linear fit (log(T) = m*log(L) + log(b)) yielded the coefficients to estimate T as T=(b)L^m.

5. *Q factor vs. Pendulum length data*

Since the manual counting method for Q factor closely matched the theoretical model (within one significant figure), I used this method for all Q factor measurements. This procedure followed the same steps as *Procedure 3* but was repeated for each pendulum length. The initial length was 0.4000 m, with a 0.0500 m reduction per trial.

RESULTS

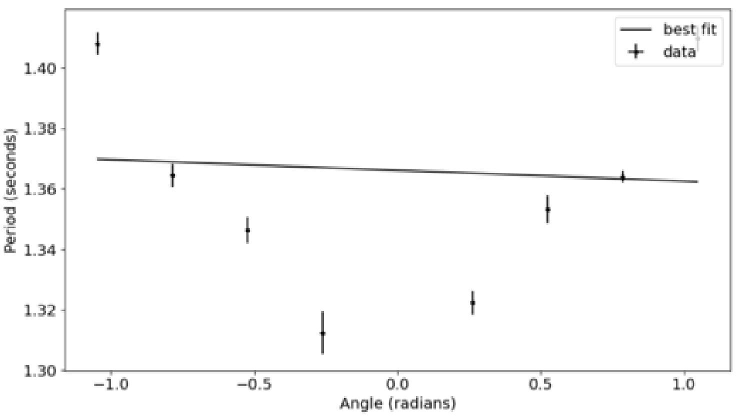

Figure 1.a: Python-generated graph of average periods (seconds) plotted against the angles (radians) at which a 14.141g mass on a 0.4000m long pendulum was released. The points are taken from both the positive side (right of 0 radians) and the negative side (left of 0 radians) of the pendulum. Horizontal error bars (±0.009 radians) are too small to be seen. A line of best fit, which is approximately flat, with equation (-0.00359±0.002) x + (1.366±0.001) passes through the graph, fitted to a linear model. The legend covers the eighth point on this graph. Residuals for this plot are included in Appendix F.

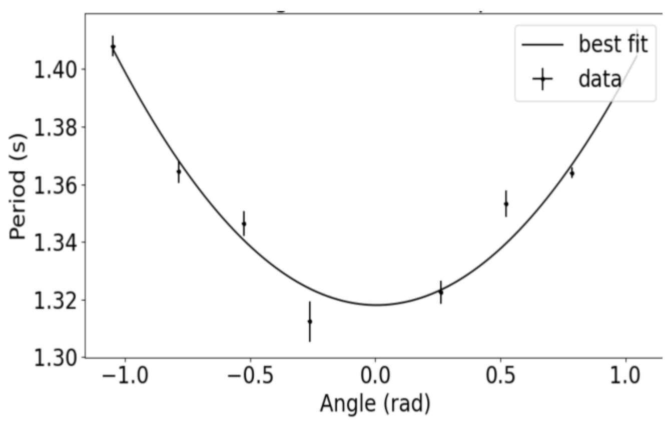

Figure 2.a: Python-generated graph of average periods (seconds) plotted against the angles (radians), where a 14.141g mass on a 0.4000m long pendulum was released. The points are taken from both the positive side of the pendulum (right of 0 radians) and the negative side (left of 0 radians). Horizontal error bars (±0.009 radians) are too small to be seen. A curve of best is drawn through the points, fitted to a quadratic model, to the equation $T = T_0(1+B\theta+C\theta^2)$, which has calculated values of T= (1.318±0.003) *((0.061±0.003) $*\theta^2$ + (-0.001±0.001) $*\theta+1$). Residuals for this plot are included in Appendix F.

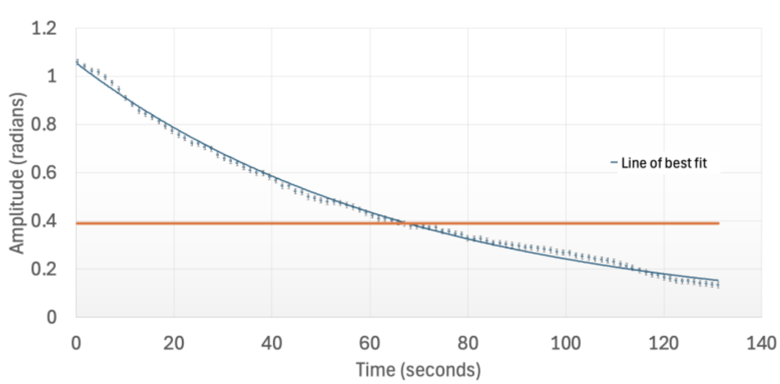

Figure 3: The amplitude (radians) of a 14.141g mass on a 0.4000m long pendulum, with an initial angle of 1.06 radians (around 60.70º), plotted against time (seconds). At this scale, the horizontal error bars (±0.004) are too small to be seen. The line of best fit of these points, the straight blue line, is an exponential function, calculated in Excel to be approximately $y=(1.06\pm0.01) *e^{(-0.0150 \pm 0.0001)\,t}$. An orange, flat line is drawn to show the equation $y = \theta_0/e$, which is calculated to be around y= (1.06±0.01)/e = 0.390±0.004, to show where about the exponential fit tau would be found.

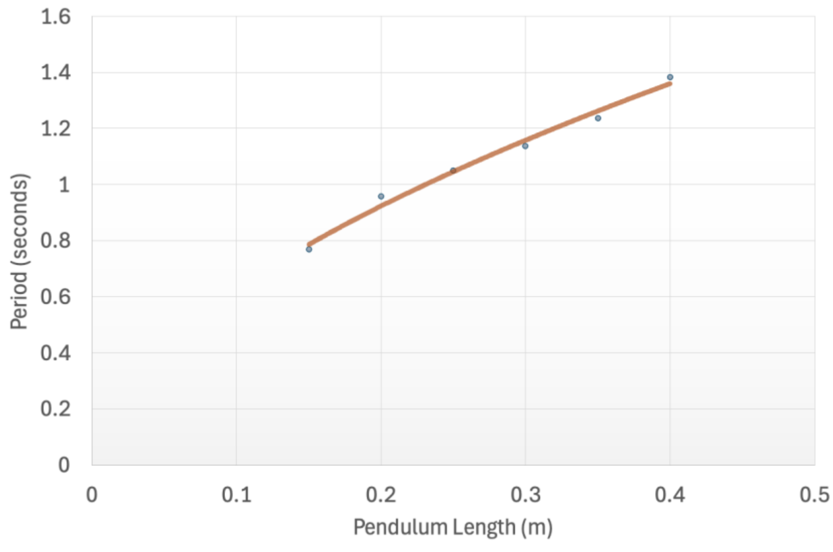

Figure 4.a: Period (seconds) plotted against pendulum length (metres), where pendulum length increases in increments of 0.005m each time. Blue dots show the data points, and the orange linear line is the line of best fit for the data points, with the equation T= $(2.3\pm0.1) * L^{(0.46\pm 0.04)}$. Error bars in the horizontal direction are too small to be seen and have a value of ±0.0005m, due to the measuring device. Error bars in the vertical direction are also too small to be seen and have values corresponding to the uncertainty between the five timed trials.

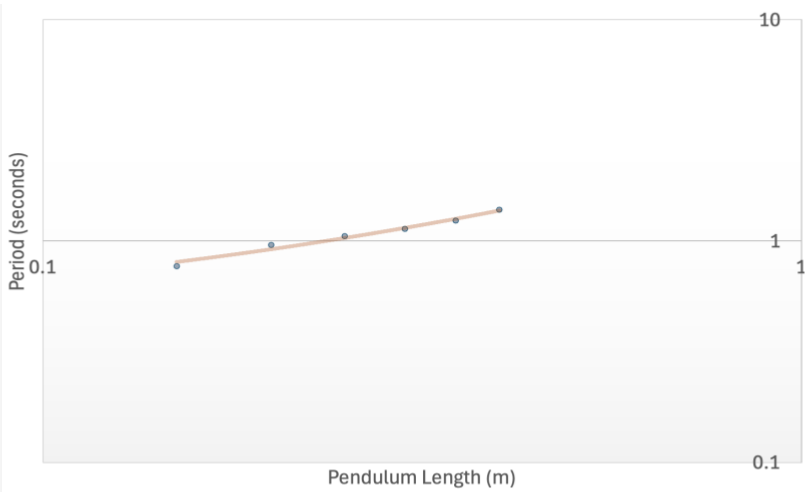

Figure 4.b: Period (seconds) plotted against pendulum length (metres) in a log-log plot. Blue dots show the data points, and the orange linear line is the line of best fit for the data points. The equation of the line of best fit is y= (0.46±0.04) *log(L) +(0.36±0.02), where y represents log(T). Error bars in the horizontal direction are too small to be seen and have a value of ±0.0005m, due to the measuring device. Error bars in the vertical direction are also too small to be seen and have values corresponding to the uncertainty between the five timed trials.

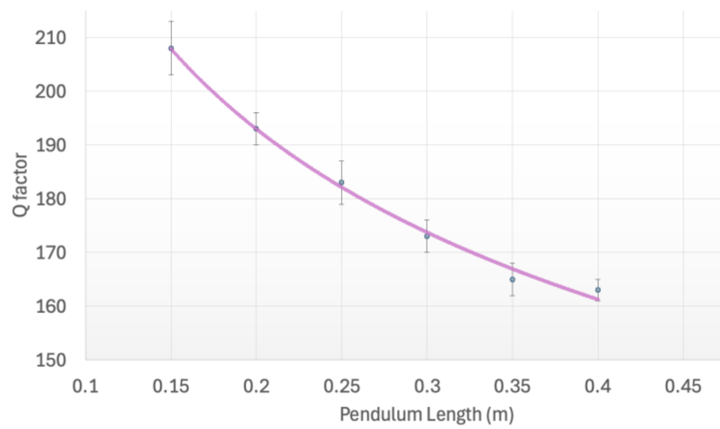

Figure 5: Q factor (unitless) plotted against pendulum length (metres). A line of best fit is plotted for the points, fitted to a power function on excel, which is the solid pink line. Its equation measures to be Q = $(127.21\pm0.01) * L^{-0.26\pm0.01}$. Error bars in the horizontal direction are too small to be seen, and have a value of ±0.0005m, due to the measuring device. Vertical error bars are visible and were calibrated through the uncertainties from counting Q factor from both the positive and negative angle direction.

UNCERTAINTIES

1. TYPE B: Horizontal error bars for *Figure 1.a* and *Figures 2.a*, and the vertical error bars for Figure 3 were ±0.009 radians because the protractor had an uncertainty of ±0.5.
2. TYPE B: Horizontal error bars for time (seconds) in *Figure* 3 were ±0.004s because the camera I used recorded at 60 frames per second, which has an error of around (1/60)/4 = ±0.004. The number 4 was arbitrarily chosen because it was the convention for frame rate uncertainty of PHY180.
3. TYPE A: Vertical error bars for amplitude (radians) in *Figure* 3 are primarily type B, given the large data set of 100 points used to fit the exponential curve. This is enough to say that type A error is negligible,

and that type B error is more prominent. Observing that most data points fell within an error bar of the fit line supports the accuracy of the exponential model.

4. TYPE A: Vertical error bars for the period (seconds) in *Figure 1.a* and *Figure 2.a* reflect type A uncertainty, where the uncertainty of the 4 different trials for each angle was taken. These values were more than the type B uncertainty, which was ±0.004, determined by the frame rate of the camera.
5. TYPE B: Horizontal error bars for length (metres) in *Figure 4.a*, *Figure 4.b,* and *Figure 5* were ±0.0005m, because the measuring device for the pendulum length was a ruler that had a precision of 0.001mm.
6. TYPE A: Vertical error bars for period (seconds) in *Figure 4.a* and *Figure 4.b* depended on the uncertainty between the 5 trials for each length. These values exceeded the frame rate-based type B uncertainty of ±0.004.
7. TYPE A: Vertical error bars for Q factor in *Figure 5* depended on the uncertainty between the 4 trials for each length for both the positive and negative side.

The largest uncertainties from my data, overall, came from the uncertainties of the different trials for the data in *Figure 1.a* and *Figure 2.a*, from the uncertainty in my Type A calculations for fitting my points to an exponential equation in *Figure 3,* and from the counting method of Q factor in *Figure 5*. Because these were all Type A uncertainties, the best thing to do to correct these uncertainties for future labs is to take more than 4 trials for each angle for *Figure 1.a* and *Figure 2.b,* to take more than 1 trial for the data for *Figure 3,* and to do more than 4 trials per positive and negative angle per pendulum length for *Figure 5*. This way, there is more of a chance that points will stray less from the median for their respective calculations.

DISCUSSION

The Q factor obtained from the counting method was 163±1, while the theoretical calculation yielded 166±4. Since the uncertainties from the calculation method and counting method are equal to 1 and 4 respectively (*see Appendix B and Appendix C for calculations*), I used the larger uncertainty, 4, to affirm whether the two Q factors are experimentally the same. The counted Q factor, with an average of 163, is less than 1 error bar less than the theoretical Q factor of 166. Therefore, the two methods for calculating the Q factor, experimentally, give the same value.

From *Figure 2.a*, T= (1.318±0.003) *((0.061±0.003) *θ^2 + (-0.001±0.001)*θ+1), where, using Equation 4 in Appendix D, B = -0.001±0.001, and C= 0.061±0.003. The value for B is consistent with zero because the uncertainty is equal to the value. However, though the value for C is very small, it is still around twenty times larger than its uncertainty, signifying that it has a measurable effect. Following Equation 5 in Appendix D, we find that the range in which C can be ignored (where $C\cdot\theta^2 \leq u(T)$) is approximately −0.257 to 0.257 radians, as calculated in Appendix E (Wilson, 2024b). Therefore, for angles within this range, T(θ) closely approximates T.

Using the linear fit in *Figure 1.a* of (-0.00359±0.002) x + (1.366±0.001), however, the slope of the line is consistent with zero because it is less than twice the value of its uncertainty. This suggests that the data does not exhibit a significant linear trend and supports the notion that angle dependence has minimal influence on period at small amplitudes.

By taking the log-log pendulum length against period data from *Figure 4.b,* which has the equation log(T)= (0.46±0.04) *log(L) +(0.36±0.02), we achieve the equation T= (2.3±0.1)* $L^{(0.46\pm 0.04)}$, as shown in *Figure 4.a*. Using the proposed model T=$2\sqrt{L}$ (Equation 2 in Appendix D), the coefficients 0.46±0.04 and 2.3±0.1, are compared to expected values of 0.5 and 2, respectively. By observing the uncertainties, the data shows that it is only partially consistent with the proposed model (Wilson, 2024a). This is because, though the value of 0.46 is within 1 error bar of 0.5, and therefore is experimentally consistent, 2.3 is 3 error bars away, which makes it less accurate to the proposed model.

Lastly, by plotting the Q factor data against the pendulum length, as shown in *Figure* 5, the equation of best fit of y = (127.21±0.01)$* x^{-0.26\pm0.01}$ was most consistent with the data points, as it passed through all of them within one error bar. This shows that the relationship between Q factor and L is Q= (127.21±0.01)$L^{-0.26\pm0.01}$.

CONCLUSION

Therefore, the data in *Figure 2.a* shows that the initial prediction of B=C=0 is wrong (*Equation 4, Appendix D)*, because C is not consistent with 0 (Wilson, 2024a). While the B value of −0.001±0.001is experimentally zero, suggesting minimal asymmetry in the pendulum's design, the non-zero C value of 0.061±0.003 indicates a slight dependence of the period on the initial angle. This is likely due to a Type A error, as not enough data was taken to reach a more accurate conclusion for the quadratic fit. An initial angle in the range of -0.257 to 0.257 radians would help achieve data that period is independent of the initial angle (*see Appendix E)*. Although the linear fit, as shown in *Figure 1.*a, shows a slope of -0.00359±0.002, which is consistent with zero, because the quadratic captures complex data patterns more precisely, the conclusion about angle dependence relies more heavily on the quadratic model.

Additionally, the Q factor attained from counting, 163±1, agrees with the Q factor achieved through the theoretical model, 166±4 to an error bar, showing that the two methods can yield consistent results. This is significant because the counting method can be used as a time-efficient alternative to the theoretical model, which streamlines data-collection more for scenarios where more trials are needed. For this reason, the counting method for Q factor was used when collecting data for the relationship between Q factor and length.

Thirdly, the proposed model of T=2$\sqrt{L}$ only partially works with the data from the pendulum, which achieved the equation T= (2.3±0.1)*$L^{(0.46\pm0.04)}$ (Wilson, 2024a). This shows that, though 0.46 is within 1 error bar of 0.5, 2.3 is 3 error bars away from 2. This suggests that using the coefficient of 2 for $\sqrt{L}$ would be inaccurate for this pendulum, and it would not fully follow T=2$\sqrt{L}$. This is likely due to Type A error, which was the largest source of error for these results and suggests that a larger number of trials may provide values more similar to the model.

Lastly, the relationship between Q factor and L was attained to be Q= (127.21±0.01)$L^{-0.26\pm0.01}$. This relationship was assumed to be decaying exponentially because the line of best fit using an exponential function passed through all the points, within 1 error bar of the collected data (*see Figure 5)*. Therefore, it can be concluded that as pendulum length increases, Q factor decreases exponentially.

Overall, the largest uncertainties in this experiment came from Type A errors and can be traced back to limited trials in measurements. This shows that a more extensive dataset would achieve a C that would experimentally be 0, which would prove that initial angle does not depend on period. Similarly, additional trials for the relationship between pendulum length and period may give results more consistent with the proposed model T=2$\sqrt{L}$. For future experiments, increasing the number of trials would lower the uncertainties, and would yield conclusions more accurate to the outlined, theoretical models.

CITATIONS (APA):

Wilson, B. (2024). PHY180 Lab Project (2024). Toronto; University of Toronto.

Wilson, B. (2024). *How to find the range of small angles*. Piazza. https://piazza.com/

Appendix A

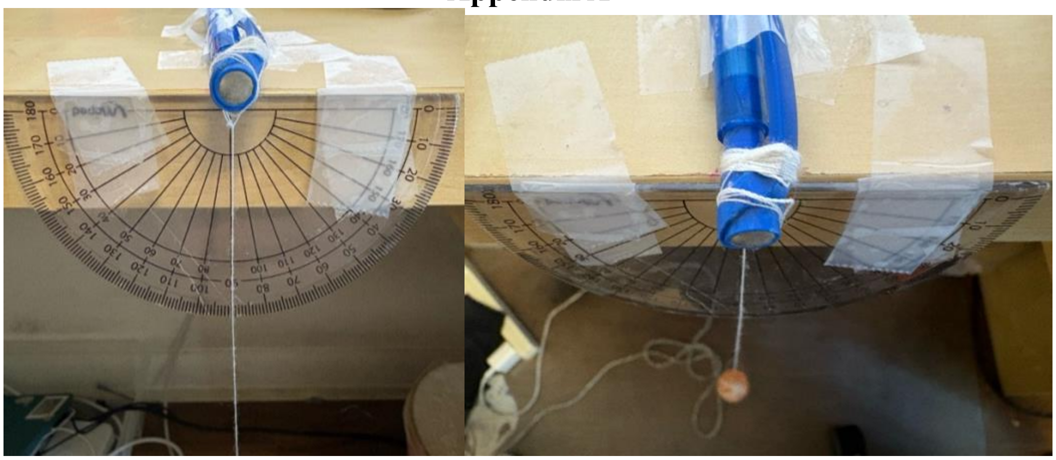

IMAGE 1a/1b: The alignment of the thread to the 90º mark of the protractor, and the protruding pencil is shown. The pencil protrudes 3.00cm from the edge of the desk.

Appendix B

	Trials	80º initial angle, positive side		80º initial angle, negative side	
		Counted oscillations	Q factor	Counted oscillations	Q factor
	1	41	164	40	160
	2	41	164	41	164
	3	41	164	41	164
	4	40	160	40	160
Average (each)		163		162	
Uncertainty (each)		1		1	
Average (total)		163			
Uncertainty (total)		1			

TABLE 1: The number of oscillations recorded, as the pendulum is released from 80º from both negative (left) and positive (right) sides, for 4 trials, until the amplitude decays to around 46% of its original amount. The average values for both the positive and negative sides for the Q factor, along with their respective uncertainties, and the average value of the total Q factor measurement, along with its uncertainty were also recorded. The maximum of the two uncertainties was taken for the total uncertainty.

APPENDIX C

To calculate the Q factor for my pendulum, I used $\theta=\theta_0*e^{-(t/\tau)}$, $Q = \pi*(\tau /T)$, and the fact that τ is when $y = \theta_0/e$ intersects the fitted model (Wilson, 2024a). From the line of best fit, by observation, $\tau =1/(0.0150\pm 0.0001)$, which is also $1/(0.0150\pm 0.6667\%) = 66.7 \pm 0.6667\%$. To see if this uncertainty is smaller or bigger than when we solve for τ, I solved for τ once, manually, using $y = \theta_0/e = 1.06/e = y=0.390\pm0.009$ and $y= (1.06\pm0.01)*e^{(-0.0150 \pm 0.0001)\ t}$:

$0.390\pm2.31\%= (1.06\pm0.943\%)*e^{(-0.0150 \pm 0.667\%)\ t}$

$t = 66.7 \pm2.31\%$

I compared this uncertainty for time with the percent of uncertainty I got from type B measurements of time. From my camera, which takes 60 frames per second, I get an uncertainty of $1/(60*4) = \pm0.004$, which is less than 2. Therefore, the uncertainty of ±0.6 is kept for time.

I used the value for tau in the equation $\theta=\theta_0*e^{-(t/\tau)}$, where $\theta =0.390\pm2.31\%$, $\theta_0=1.06\pm0.943\%$, $t=66.7 \pm2.31\%$:

$0.390\pm2.31\%= (1.06\pm0.943\%)*\ e^{(66.7\ \pm2.31\%)/\tau}$

$\tau = 66.77\pm2.31\% = 67\pm2$.

This value of uncertainty is larger than the initial one, so $\tau = 67\pm2$ will be used. From here, I used the formulas for $Q = \pi*(\tau /T)$ and $T \simeq 2\sqrt{(L)}$ to calculate Q factor (Wilson, 2024a). The length of the pendulum was 0.4000m, and the measuring device had an uncertainty of 0.0005m. From this, the length is 0.4000m ±0.125.

Therefore, $T = 2\sqrt{(L)} = 2\sqrt{(0.4000 \pm0.125\%)} = 1.26 \pm 0.125\%$

$Q = \pi*(\tau /T) = \pi*(66.7\pm2.31\% /1.26 \pm 0.125\%) = 166.3 \pm2.31\% = 166\pm 4$

APPENDIX D

Equation 1: $$\theta(t) = \theta_0\ \mathrm{e}^{-t/\tau} \cos\left(2\pi\frac{t}{T} + \phi_0\right)$$ (Wilson, 2024a)

Equation 2: $$T \simeq 2\sqrt{L}$$ (Wilson, 2024a)

Equation 3: $$Q = \pi\frac{\tau}{T}.$$ (Wilson, 2024a)

Equation 4: $$T = T_0(1 + B\theta_0 + C\theta_0^2 + \ldots)$$ (Wilson, 2024a)

Equation 5: $T(\theta)=T_0+C\theta^2$ (Wilson, 2024a)

APPENDIX E

Maximum uncertainty of period was taken to be ±0.004s, from the frame rate uncertainty, because this value was greater than all other uncertainties measured for period. Using Equation 5 in Appendix D, and the fact that $C\theta^2\leq u(T)$ which is $(0.061)\theta^2\leq0.004$, θ would have to be between -0.257 to 0.257 radians for period to not depend on initial angle.

APPENDIX F

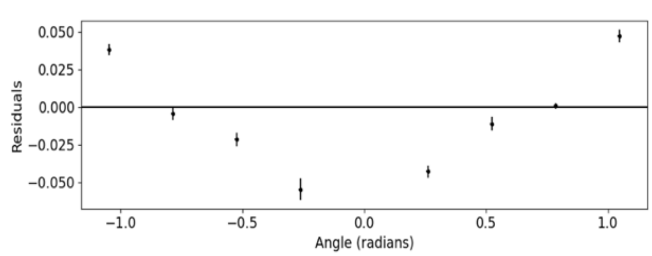

Figure 1b: The residuals of the period (s) against angle (radians) values from *Figure 1.a* are shown. The points exhibit a parabolic spread around the 0-line, due to the small scale of the vertical axis. Most of these values are not within 2 standard deviations of the 0-line, showing that this linear fit does not give a good estimate of a bell curve.

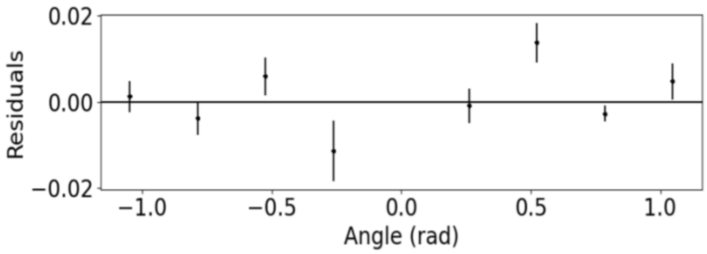

Figure 2.b: The residuals of the period (s) against angle (radians) values from *Figure 2.a* are shown. Approximately 5/8 of the points are almost within an error bar of 0, showing that this is close to a bell curve estimate, but may need more points for a firmer conclusion.